Proteomics and gene expression analyses of squalene-supplemented mice identify microsomal thioredoxin domain-containing protein 5 changes associated with hepatic steatosis

Adela Ramírez-Torres[1], Sílvia Barceló-Batllori[2], Roberto Martínez-Beamonte[1, 5], María A. Navarro[3, 5], Joaquín C. Surra[1, 5], Carmen Arnal[4, 5], Natalia Guillén [1, 5], Sergio Acín[3, 5], Jesús Osada[1, 5]

[1]Departamento Bioquímica y Biología Molecular y Celular, Facultad de Veterinaria, Instituto de Investigación Sanitaria de Aragón (IIS), Universidad de Zaragoza, Spain

[2]Unidad de Proteómica, IIS Aragón. Zaragoza, Spain

[3]Unidad de Investigación Traslacional. IIS Aragón. Hospital Universitario Miguel Servet. Zaragoza, Spain

[4] Departamento de Patología Animal, Facultad de Veterinaria, Universidad de Zaragoza, Spain

[5]CIBER de Fisiopatología de la Obesidad y Nutrición, Instituto de Salud Carlos III, Spain

Correspondence to: Jesús Osada, PhD,
Department of Biochemistry and Molecular Biology,
Veterinary School, University of Zaragoza,
Miguel Servet, 177, E-50013 Zaragoza, Spain.
Fax number: 34-976-761612
Telephone number: 34-976-761644
E-mail: josada@unizar.es

Abstract

Squalene is an abundant hydrocarbon present in virgin olive oil. Previous studies showed that its administration decreased atherosclerosis and steatosis in male apoE-knock-out mice. To study its effects on microsomal proteins, 1 g/kg/day of squalene was administered to those mice. After 10 weeks, hepatic fat content was assessed and protein extracts of microsomal enriched fractions from control and squalene-treated animals were analyzed by 2D-DIGE. Spots exhibiting significant differences were identified by peptide fingerprinting and MSMS analysis. Squalene administration modified the expression of thirty-one proteins involved in different metabolic functions and increased the levels of those involved in vesicle transport, protein folding and redox status. Only mRNA levels of 9 genes *(Arg1, Atp5b, Cat, Hyou1, Nipsnap1, Pcca, Pcx, Pyroxd2,* and *Txndc5)* paralleled these findings. No such mRNA changes were observed in wild-type mice receiving squalene. Thioredoxin domain-containing protein 5 (TXNDC5) protein and mRNA levels were significantly associated with hepatic fat content in apoE-ko mice. These results suggest that squalene action may be executed through a complex regulation of microsomal proteins, both at the mRNA and post-transcriptional levels and the presence of apoE may change the outcome. *Txndc5* reflects the anti-steatotic properties of squalene and the sensitivity to lipid accumulation.

Keywords: apoE-knock-out mice, fatty liver, squalene, proteomics, microsomes, thioredoxin domain-containing protein 5, TXNDC5, endoplasmic reticulum

Introduction

Non-alcoholic fatty liver disease (NAFLD) or hepatic steatosis has become a burden disease in Western societies paralleling the prevalence of obesity [1]. While most patients do not progress to further complications, a few of them develop a spectrum of liver pathologies such as steatohepatitis, cirrhosis and hepatocellular carcinoma [2, 3]. Hepatic steatosis is an entity not only compromising lipid metabolism [4], but also inducing whole genome expression changes [5] demanding high-throughput approaches for its study. Therefore, given the prevalence of this pathological entity and its potencial complications, it is critical to know its mechanisms to find new therapies in its early stages.

Administration of olive oil, main source of dietary fat in the traditional Mediterranean dietary pattern, has shown to improve NAFLD as shown in apoE- deficient mice by decreasing hepatic triglyceride accumulation [6], an effect mainly attributed to its monounsaturated fatty acid content [7]. However, administration of different virgin olive oils showed changes at the proteomic level and in the degree of hepatic steatosis that were not directly related to its oleic acid content [8]. A potential explanation for this observation could be that virgin olive oil is a complex mixture containing saponifiable and unsaponifiable fractions [9], and for the latter, biological actions have been documented [10-13]. Squalene, as major component of the unsaponifiable fraction, may vary from 1.5 to 9.6 g/ kg in different virgin olive oils [14]. Likewise, the human average intake of squalene ranges from 30 up to 400 mg/day (United States and Mediterranean countries, respectively) [15] or even 1g per day in some diets [16]. Due to its low toxicity, it has been successfully used to treat different ailments [17, 18]. Our group has shown that a high squalene dose decreased hepatic fat content in a sex-dependent manner [19] in apoE-deficient mice, a well-characterized and widely used

74 animal model which rapidly develops atherosclerotic lesions similar to those observed
75 in humans [20]. ApoE deficiency in these animals leads to a moderate or severe hepatic
76 steatosis when fed standard chow or a high fat diet, respectively [21, 22]. The hepatic
77 fat content has been associated with the development of atherosclerotic lesions [23] and
78 modulated by dietary interventions [6, 24].

79 The endoplasmic reticulum (ER) is a multifunctional organelle involved in several vital
80 functions including protein synthesis, processing and folding, intracellular transport and
81 calcium signaling, drug detoxification and lipid metabolism [25]. Disturbed homeostasis
82 in the ER, caused by high levels of free fatty acid, depletion of calcium or insulin
83 resistance, leads to accumulation of misfolded proteins, which triggers a stress response,
84 commonly known as the unfolded protein response (UPR). It has been shown that ER
85 stress participates in the pathogenesis of hepatic steatosis, insulin resistance, obesity and
86 diabetes [26-28]. Since endoplasmic reticulum plays a central role in lipid catabolism,
87 and squalene decreases hepatic fat content, our hypothesis was that squalene
88 administration could modify hepatic microsomal proteins linked to hepatic steatosis. To
89 address such issues and gain more insight into the mechanisms involved in the action of
90 dietary squalene supplementation, 2D-DIGE analysis was used to study the
91 modifications caused by squalene in apoE-ko mice. Firstly, microsomal fractions were
92 obtained by differential centrifugation. Secondly, proteomic experiments were
93 performed to separate proteins. Using gel image analysis, differences in protein
94 expression between both experimental conditions were searched. Those proteins
95 displaying significant differences were identified by mass spectrometry and considered
96 putative squalene targets. Thirdly, their expression changes were analyzed at the mRNA
97 level. Finally, the candidate genes were also examined in wild-type and apoA1-ko mice.
98 In all experiments groups of squalene- and chow-fed animals were used to distinguish

the solely squalene administration effects in these animals from those related to fatty liver present in the apoE-ko mice which were modified by administrating this compound.

2. Methods and materials

2.1. Animals and diets.

Male homozygous apoE-ko mice, hybrids of C57BL/6JxOla129 strains (more than 95% on Ola129 based on plasma cholesterol and apolipoproteins, and color coat), aged 2 months were randomly distributed into two experimental groups matched on their baseline plasma cholesterol values: the squalene group (n=5) whose beverage contained 1% (v/v) of squalene in glycerol solution and the control group (n=5), which received glycerol solution, used as vehicle. The squalene dose was 1 g/kg/day and the administration lasted 10 weeks as previously described [19]. Both groups were daily fed with mice chow, Teklad Mouse/Rat Diet no. 2014 (Harlan Ibérica, Barcelona Spain). A second experiment was carried out in two groups of male C57BL/6J wild-type mice: control (n=6) and squalene (n=7) and a third experiment was undertaken in male apoA1-ko mice on C57BL/6J genetic background receiving chow diet (n=7) and squalene (n=7). In these experiments, squalene regimen was well tolerated as there was no incidence on survival, physical appearance and solid and liquid intakes. At the end of the 10-week intervention period and after an overnight fast, the animals were killed by suffocation with CO_2 and blood was obtained thereafter by cardiac puncture. The livers were removed, weighed, frozen in liquid nitrogen, and stored at -80º C until analysis. The protocol was approved by the Ethics Committee for Animal Research of the University of Zaragoza.

2. 2. Measurement of hepatic fat

Paraffin-embedded liver sections (4 μm) were stained with hematoxylin and eosin and observed using a Nikon microscope. The extent of fat droplets in each liver section was evaluated with Adobe Photoshop CS and expressed as percentage of total liver section.

The diameter of 100 fat droplets of each mouse was also measured by means of Scion Image software (Scion Corporation, Frederick, Maryland, USA).

2.3. Preparation of microsomal fraction

This fraction was prepared and characterized according to Osada et al. [29]. Livers from apoE-ko mice were homogenized in PBS (4 ml/g of tissue) with protease inhibitor cocktail tablets (Roche) using a Potter homogenizer. Debris tissue was removed by centrifugation at 200 g for 10 min at 4ºC. The homogenate was spun down at 1000 x g for 15 min. The supernatant containing mitochondria was centrifuged at 13000 g for 2 min. Centrifugation of the post mitochondrial supernatant at 105000 g for 90 min yielded the microsomal pellets which were washed twice, spun at the same speed and finally resuspended in 0.5 ml of PBS. Sample preparation for DIGE analysis was done as described previously [30] and protein content was quantified using the RC/DC Protein Assay (Bio-Rad Laboratories).

2.4. 2D-DIGE electrophoretic analyses

Microsomal protein samples from apoE-deficient mice (five biological replicates of each experimental condition) were analyzed by 2D-DIGE minimally labeled with Cy3 and Cy5 fluorescent dyes (50 µg of protein/400 pmol of dye) as previously described [30]. An internal standard was prepared by mixing equal amounts of microsomal proteins from control and squalene groups labeled with Cy2. Two-dimensional electrophoresis was carried as recently described [31] using 50 µg of each Cy2-, Cy3- and Cy5-labeled samples. Fluorescence images of the gels were acquired using a Typhoon Trio 9000 scanner (GE Healthcare) and processed using ImageQuant TM TL Software (GE Healthcare). Determination of protein spot abundance was performed

153 using the Progenesis SameSpots v4.0 software (Nonlinear Dynamics, U.K.). For protein
154 identification, a preparative gel including 500 μg of microsomal protein (50 μg Cy2
155 labeled as internal standard) was also performed and stained with Coomassie. Spots
156 whose densities significantly differed between treatments were excised manually from
157 the preparative gel and subjected to triptic digestion as described [31].
158
159 **2.5. Mass spectrometry analyses**

160 Sample and matrix, a saturated solution of alpha-cyano-4-hydroxycinnamic acid in 50%
161 ACN/0.1% TFA/H_2O, were spotted in duplicate onto an Opti-Tof 384 well insert plate
162 (Applied Biosystems). MALDI-TOF MS was performed using a 4800plus MALDI-
163 TOFTOF (Applied Biosystems) in the reflector mode with accelerating voltage of 20
164 kV, mass range of 800 to 4000 Da and 1000 shots/spectrum. MS/MS spectra were
165 acquired automatically on the 20 most intense precursors and calibrated using a standard
166 protein mixture (4700 Calmix, Applied Biosystems). Alternatively, samples were dried
167 and resuspended in 0.1 % formic acid and analysed by LC-MSMS in a nanoAcquity
168 (Waters) coupled to an OrbitrapVelos (Thermo Scientific). Sample was injected in a
169 C18 phase reverse column (75 μm Øi, 10 cm, nano Acquity, 1.7μm BEH column,
170 Waters) in a gradient 1-40% for 20 min and 40-60% for 1 min at a flow rate of
171 250nl/min (A: 0.1% formic acid; B: 0.1% acid formic in acetonitrile). Eluted peptides
172 were ionized by ESI (PicoTipTM, New Objective 2000V). Peptide masses were
173 analyzed in the Orbitrap in full scan (m/z 350-1700) and 5 most abundant peptides were
174 selected for CID fragmentation using helium as collision gas. Data was extracted with
175 software Thermo Xcalibur (v.2.1.0.1140).
176
177 **2.6. Protein identification and data-mining**

178 Proteins were identified using Mascot (Matrix Science Ltd.) with the SwissProt
179 database 57.15. MS/ MS data were searched according to the following criteria: fixed
180 modifications carbamidomethyl (cysteines) and peptide tolerance of 0.1 Da, fragment
181 mass tolerance of 0.3 Da, one missed cleavage and against the SwissProt Database for
182 mammalian proteins (64838 sequences). Proteins with a score above 61 ($P<0.05$) were
183 considered as a positive hit. The Protein Analysis Through Evolutionary Relationships
184 (PANTHER) resource was used to classify data into different categories
185 (www.pantherdb.org). Biological function was annotated using a manual elaboration of
186 information available at the following sites accessed on May 17th, 2012:
187 http://www.ebi.ac.uk/gxa/gene/
188 http://www.ncbi.nlm.nih.gov/sites/entrez?db=gene&cmd=
189 http://func.mshri.on.ca/mouse/genes/list_functional_scores/102773
190 http://www.informatics.jax.org/javawi2/servlet/WIFetch?page=markerQF
191 http://vega.sanger.ac.uk/Mus_musculus/Gene/
192
193 **2.7. Quantitative PCR analyses.**
194 RNA from 100-mg liver mice was extracted using TriReagent (Sigma). DNA
195 contaminants were eliminated using the DNA removal kit from AMBION (Austin, TX,
196 USA). First-strand cDNA synthesis (0.5 μg) and PCR reactions were performed using
197 the SuperScript II Platinum Two-Step RT-qPCR Kit with SYBR Green (Invitrogen,
198 Madrid, Spain) as previously described [19]. The mRNA expression was analyzed by
199 quantitative real time PCR (qPCR) of individual samples using equal amounts of RNA.
200 The primers (Supplementary Table 1) according to MIQE guidelines [32] were
201 designed using Primer Express software (Applied Biosystems, Foster City, CA). The
202 relative quantification of gene expression was analyzed by the $2^{-\Delta\Delta Cq}$ method [33]. The

mRNA expression corresponding to the *cyclophilin B* was used as the reference control.

2.8. Statistical analyses

Data were processed using SPSS version 20.0 software (SPSS®, Chicago, IL). Comparisons were carried out using Mann–Whitney *U*-test. Correlations between variables were tested by calculating the Spearman's correlation coefficient. Significance was set at $P < 0.05$.

3. Results

3.1. Histological analyses

ApoE-ko mice accumulate triglycerides and cholesterol in liver [34]. Although squalene did not modify plasma cholesterol and triglycerides [19], male apoE-ko mice receiving this agent showed decrease of hepatic fat content. Representative images are shown in Figure 1, panels A and B, and quantitative assessment showed that the decrease was statistically significant (Fig. 1C)**.** Indeed, lipid droplet size was found significantly decreased in squalene-supplemented mice (control 2.16 ± 0.02 vs squalene group 2.08 ± 0.03 μm**;** Fig.1D). The tiny decrease in lipid droplet size compared to the important decrease in size occupied by lipids is suggesting a decrease in the number of lipid droplets as the main effect of squalene.

3.2. Microsomal proteomic profile after the dietary supplementation of squalene in apoE-ko mice

The specific activity of the microsomal marker enzyme NADPH cytochrome P450 reductase used to monitor the purification process revealed an enrichment of over 3-fold and a yield of fraction recovery of over 28%. No enrichment was found when specific succinate dehydrogenase activity was used as mitochondrial marker and yield of this enzyme was lower than 9%. Separation and identification of microsomal hepatic proteins differentially regulated by squalene supplementation were carried out by 2D-DIGE. SameSpots software revealed statistically significant differences in 34 protein spots using ANOVA ($p<0.05$). Subsequently, after running a preparative Coomassie-stained gel (Figure 2), including cy2-labeled proteins, the selected spots were manually excised and identified by MALDI-MS, being the hits searched in the databases (Table 1 and Supplementary Table 2). Twenty-two protein spots showed at least 1.3-fold

237 increased expression in the squalene group compared to the control group, while twelve
238 protein spots were 1.3-fold decreased (Table 2). We observed changes in 10 proteins
239 corresponding to mitochondria, 3 to peroxisomes and 19 to reticulum. Using protein
240 accession numbers and PANTHER gene ontology database [35], proteins were
241 classified in two groups according to their 1) biological processes or 2) molecular
242 functions. Attending to the biological process criteria, protein changes were grouped in
243 5 categories (Fig. 3A), the majority of which participated in metabolism (46%). Of
244 these, 68% were involved in primary metabolic processes (Fig. 3A), that is, protein and
245 lipid (53%), amino acid (17%), nucleic acid (17%) and carbohydrate metabolism (13%).
246 Attending to their molecular functions (Fig. 3B), the 61% of the differentially expressed
247 proteins showed catalytic activity mainly as oxidoreductases (30%), hydrolases (20%),
248 transferases (17%) and isomerases or ligases (13% each, respectively). A more detailed
249 classification based on biological functions and subcellular localizations is shown in
250 Table 2. In mitochondrial proteins those involved in generation of oxalacetate (PYC,
251 *Pcx*), fatty oxidation (*Echs1* and *Pcca*) and generation of ATP (*Atp5a1* and *Atp5b*) were
252 increased while catabolism of amino acids and generation of urea (*Glud1* and *Cps1*)
253 were decreased. For peroxisomes some isoforms of fatty oxidation and inactivation of
254 hydrogen peroxide were increased (*Acox1* and *Cat*). In reticulum, proteins involved in
255 catabolism of amino acids (*P4hb* and *Ftcd*) and folates (*Aldh1l1*) were decreased,
256 except arginine catabolism (*Arg1*), and amino acid biosynthesis (*Pbld2*) was increased.
257 Proteins involved in lipid (*Mup8* and *Scp2*) and vesicular transport (*Nipsnap1* and *Vcp*),
258 quality control of proteins (*Psma7, Pdia3, Hyou1* and *Hspa5*), calcium storage (*Calr*)
259 and redox homeostasis (*Txndc5 and Pyroxd2*) were increased. Overall, squalene
260 administration seems to favor an environment of protein biosynthesis and stabilization
261 along with calcium storage and control of redox status in endoplasmic reticulum.

3.3. RNA analysis of differentially expressed proteins

In order to support the observed squalene-induced protein changes, mRNA expression analyses by qPCR of the 31 identified gene products were carried out in apoE-ko mice. *Aldh1l1, Arg1, Atp5b, Cat, Cps1, Hyou1, Ndufs1, Nipsnap1, Pcca, Pcx, Pyroxd2, Slc25a13* and *Txndc5* mRNA levels displayed significant increases after squalene supplementation (Table 2). While changes in *Arg1, Atp5b, Cat, Hyou1, Nipsnap1, Pcca, Pcx, Pyroxd2,* and *Txndc5* paralleled the findings observed in the proteomics analysis (Table 2), for *Aldh1l1, Cps1, Ndufs1* and *Slc25a13* an opposite behavior was observed. For the remaining 18 gene products, the changes at the protein level were not accompanied by mRNA changes. The fact corroborates that protein and mRNA expression levels do not always show a direct correlation, since protein turnover rate, stability, degradation, processing and post-translational modifications are not reflected at the mRNA level [36]. There were evidences of post-translational modifications in the identified proteins because of the deviations from the experimental pI, estimated by spot migration in the 2D gels, and their corresponding theoretical values (vg CATA [spot 5] and CPSM [spots 23-26], Table 1). Indeed, post-translational modifications such as acetylation and phosphorylation of CPSM have already been described [37] [38]. Further work will be required to identify the post-transcriptional and post-translational mechanisms underlying the observed changes at the protein level and not in mRNA abundance.

To verify whether the mRNA changes in response to squalene were independent of the presence of apolipoprotein E, wild-type animals were fed squalene, and the nine hepatic transcripts reproducing the protein pattern were assayed. In this experimental setting of presence of apoE (Table 3), squalene administration only produced a significant

287 decreased expression of *Hyou1*, while *Arg1, Atp5b, Cat, Nipsnap1, Pcca, Pcx, Pyroxd2*
288 and *Txndc5* expressions did not experience significant changes.

289 The requirement of squalene for *Hyou1* mRNA changes was also tested in mice lacking
290 *Apoa1* as genetic model of absence of HDL and low possibility to deliver the
291 hydrophobic molecule, squalene, to the liver [39]. Interestingly, these mice showed no
292 change for *Hyou1* (data not shown). Collectively, these results suggest that the absence
293 of apoE is an important determinant of squalene action and that *Hyou1* expression is
294 sensitive to squalene administration.
295
296 **3.4. Association among protein and mRNA expression changes and hepatic fat**
297 **accumulation**
298 The likelihood that protein expression could be associated with changes in hepatocyte
299 fat accumulation induced by squalene intake in apoE-ko mice was analyzed by a
300 correlation study among differences in levels of protein expression (% normalized spot
301 volume) and the hepatic fat content. As reflected in Figure 4A, an inverse and
302 statistically significant correlation was found between hepatic fat content and
303 thioredoxin domain-containing protein 5 (TXNDC5) levels. No association was found
304 between protein levels and diameter of lipid droplets (data not shown). T*xndc*5 mRNA
305 changes were also inverse and significantly associated with hepatic fat (Fig. 4B). Since
306 TXNDC5 changes were reflected at its mRNA level, an analysis of association was also
307 carried out among this messenger changes and the other transcript levels in apoE-Ko
308 mice. As shown in Fig. 4C, when a correlation analysis among *Txndc*5 and other hepatic
309 mRNA levels was carried out, its mRNA levels were found significantly correlated
310 with those of *Aldh1l1, Arg1, Cps1, Cat, Hyou1, Ndufs1, Pcx* and *Slc25a13*. These
311 results indicate that *Txndc5* expression is associated with that of these other genes.
312

4. Discussion

In this study, the possible molecular mechanisms involved in hepatic steatosis have been investigated by studying the effects of administration of squalene, the major compound of the unsaponifiable fraction in virgin olive oil. For this purpose, liver microsomal proteomes from standard chow-fed apoE-ko mice supplemented or not with squalene have been analyzed and compared. Using 2D-fluorescence DIGE gels and image processing, thirty one proteins displaying significant differences were identified by mass spectrometry and considered putative squalene targets. Their changes were studied at the mRNA level and nine of them *(Arg1, Atp5b, Cat, Hyou1, Nipsnap1, Pcca, Pcx, Pyroxd2,* and *Txndc5)* paralleled the findings observed in the proteomics analysis. TXNDC5 also showed protein and mRNA levels associated with the degree of fat content in the liver. When these nine candidate genes were analyzed in squalene-fed wild-type animals, only *Hyou1* expression showed a significant decrease. The sensitivity of *Hyou1* changes to squalene was also tested in *Apoa1*-deficient mice and its expression did not change. Using these animal models has allowed us to differentiate between the effects of squalene administration with or without fatty liver, developed by absence of apoE, and to define expression changes of squalene-sensitive genes.

Our proteomics approach unveiled thirty one proteins displaying significant differences. The mild effects are consistent with our previous experiences in the field using one dietary component [31, 40] or complex mixtures such as virgin olive oils [8], and those of others [41] [12] indicating the inherent characteristics of dietary interventions in the nutrition field. Observed changes covered all aspects of metabolism, being particularly relevant those belonging to protein and lipid pathways (53% of changes), which are consistent with the important role of endoplasmic reticulum in these metabolic processes [25]. In addition, the administration of this

agent increased proteins involved in all actions of reticulum such as lipid and vesicular transport, protein quality control, calcium storage and redox homeostasis. Particularly the increase in GRP78/HSPA5 and PDIA3, known chaperones of apoB100 [42], could be relevant to control apoB100 insertion in VLDL, secretion of these particles and hepatic steatosis.

The presence of mitochondrial proteins in microsomal preparation could represent a special contamination between these fractions in the preparation. The facts that no special enrichment of microsomes by mitochondria according to succinate dehydrogenase activity and that some mitochondrial proteins increased while other decreased are indicative of selective changes in these proteins induced by squalene rather than contamination. Something not surprising taking into account that most mitochondrial proteins are biosynthesized outside these organelles and need to be transferred into them, and close interaction between both subcellular fractions also exists [43, 44]. In fact, carbamoyl phosphate synthetase 1 (CPSM or CPS1) was copurified with 10-formyltetrahydrofolate dehydrogenase (ALDH1L1/ FDH) and betaine homocysteine S-methyltransferase as a protein complex of 300 kDa in rat [45]. Likewise, the presence and opposite nature of changes noted for peroxisomal proteins in our preparations could be explained by the dependence of peroxisomes on the microsomal protein biosynthesis [46, 47].

Another important finding of this study was the increased thioredoxin domain containing 5 (TXNDC5) protein expression in apoE-ko mice receiving squalene and that both its protein and mRNA levels were also significantly associated with hepatic fat content. TXNDC5 belongs to the thioredoxin family, has a protein disulphide isomerase-like domain which is thought to catalyse disulphide formation to aid protein folding or to regulate protein function against endoplasmic reticulum stress induced by

363 oxidative insults [48]. Interestingly, an important decrease in oxidative stress,
364 evaluated as 8-isoprostaglandin$F_{2\alpha}$, was observed in mice receiving squalene [19], in
365 agreement with previous reports [49]. So, these protein changes could contribute to this
366 lower oxidative stress. Furthermore, oxidative stress has been shown to induce apoB
367 degradation [50] [51] and in this way decreased VLDL secretion. The observed
368 association of TXNDC5 with the degree of fatty liver opens an interesting role for this
369 protein in control of apoB in fatty liver present in absence of apoE. Furthermore,
370 squalene-induced increase in TXNDC5 expression was also at the mRNA level in
371 apoE-ko mice and these changes were in association with other members of ER
372 mRNAs suggesting a coordinated regulation. In wild-type mice, this mRNA was not
373 modified by squalene administration (Table 3). Thus, TXNDC5 seems a marker of the
374 hepatic steatosis developed in absence of apoE and may play a role in this condition's
375 amelioration induced by squalene.
376 HYOU1 levels were found increased in apoE-deficient mice receiving squalene and
377 their changes were correlated with their mRNA. HYOU1/GRP170/ORP150 mediates
378 efficient insertion of polypeptides into the microsomal membrane using nucleoside
379 triphosphates [52]. In addition to this role, it may participate in cell signalling. In this
380 regard, HYOU1 or ORP150 is up-regulated by hypoxia, its expression increased in
381 glucose starved cells [53], decreased in calorie-restricted mice [54] and had a role in
382 hepatic insulin action [55, 56]. Transgenic mice overexpressing ORP150 showed lower
383 concentrations of serum triglyceride, glucose and insulin [57]. In addition, it has been
384 considered as an inhibitor of apoptosis in hepatocytes [58]. Based on these properties,
385 squalene induction of this protein, which may protect hepatocytes, takes place at
386 mRNA level. However, it is dependent on the presence of apoE since its increase was
387 not observed in wild-type mice. In addition it requires the transport of high density

388 lipoproteins to the liver since mice lacking apoA1 failed to show any effect. These
389 findings open interesting possibilities regarding the effects of squalene in more
390 advanced liver diseases, which would be particularly attractive considering its low
391 toxicity.
392 An interesting observed aspect was the decrease in fat content through decrease in
393 number and size of lipid droplets by squalene administration (Figure 1). A decrease that
394 was found associated with decreased atherosclerosis lesion [19]. Likewise, presence of
395 increased hepatic lipids and atherosclerosis has been widely reported in mice [24, 59],
396 rabbits [60] and even in humans [61]. However, increased hepatic lipids have been also
397 associated with lower atherosclerosis [8]. In latter case, the increased antioxidant
398 defence was considered as a potential explanation for the outcome, and as a common
399 finding for both conditions of hepatic fat changes might be an important player. But the
400 picture will be more complex, our male mice receiving squalene accumulate it in liver
401 [19]. Recently, using yeasts that accumulate squalene, it has been proposed that this
402 compound can be accommodated in lipid droplets or organelle membranes without
403 causing deleterious effects [62]. Overall, these observations are in line with current
404 opinion of whether non-alcoholic fatty liver disease is a defence mechanism against
405 toxic fatty acids [5] that may became awry under some circumstances, and squalene as
406 modulator of hepatic fat content that needs to be studied in depth.

407 In conclusion, proteomic experiments in apoE knockout mice point out that squalene
408 action is modifying endoplasmic reticulum proteins participating mainly in lipid and
409 protein metabolisms, more specifically, increasing proteins involved in lipid and
410 vesicular transport, protein quality control, calcium storage and redox homeostasis.
411 When the protein changes were studied at the mRNA level, nine of them *(Arg1, Atp5b,*
412 *Cat, Hyou1, Nipsnap1, Pcca, Pcx, Pyroxd2,* and *Txndc5)* paralleled the findings

observed in the proteomics analysis. Their mRNA levels were up-regulated by squalene administration in an apoE-dependent way. TXNDC5 protein and mRNA changes were associated with the degree of fatty liver developed by absence of apoE. The variation in TXNDC5 expression in presence of fatty liver was associated with the beneficial effect of squalene, suggesting a novel role for this protein in steatosis development.

Acknowledgments

This research was supported by grants from CIBER Fisiopatología de la Obesidad y Nutrición as an initiative of FEDER- ISCIII, FEDER-CICYT (SAF 2010-14958), *Redes* FSE-DGA (B-69) and *Gobierno de Aragón* (PI025/08). We thank Irene Orera from the *Unidad de Proteómica* of IIS and Eliandre de Oliveira from *Plataforma de Proteómica* (Parc Cientific de Barcelona-ProteoRed-ISCIII). A.R. was recipient of a *Gobierno de Aragón* grant. No competing financial interests exist.

Abbreviations

ACOX1, Acox1, peroxisomal acyl-coenzyme A oxidase 1; ACTB, *Actb*, actin, cytoplasmic 1; AL1L1, Aldh1l1, aldehyde dehydrogenase family 1 member L1; ARGI1, *Arg1*, arginase-1; ATPA, *Atp5a1*, ATP synthase subunit alpha, mitochondrial; ATPB, *Atp5b*, ATP synthase subunit beta, mitochondrial; CALR, *Calr*, Calreticulin; CATA, Cat,catalase; CMC2, *Slc25a13*, calcium-binding mitochondrial carrier protein Aralar2; COQ9, *Coq9*, ubiquinone biosynthesis protein COQ9, mitochondrial; CPSM, *Cps1*, carbamoyl-phosphate synthase [ammonia], mitochondrial; DHE3, *Glud1*, glutamate dehydrogenase 1, mitochondrial; ECHM, *Echs1*, enoyl-CoA hidratase; EST31, *Ces3a*, liver carboxylesterase 31; FTCD, *Ftcd*, formimidoyltransferase-cyclodeaminase; GRP78, *Hspa5*, 78 kDa glucose-regulated protein; GSTM1, *Gstm1*, glutathione S-transferase Mu 1; HYOU1, *Hyou1*, hypoxia up-regulated protein 1; LDL, low density lipoprotein; MIQE, minimum information for publication of quantitative real time PCR experiments; MUP8, *Mup8*, major urinary proteins 11 and 8; NDUS1, *Ndufs1,* NADH-ubiquinone oxidoreductase 75 kDa subunit; NIPS1, *Nipsnap1*, protein NipSnap homolog 1; NLTP, *Scp2*, non-specific lipid-transfer protein; PANTHER, protein analysis through evolutionary relationships; PBLD2, *Pbld2*, phenazine

444 biosynthesis-like domain-containing protein 2; PCCA, *Pcca*, propionyl-CoA
445 carboxylase alpha chain, mitocondrial; PDIA1, *P4hb*, Protein disulfide-isomerase;
446 PDIA3, *Pdia3*, protein disulfide-isomerase A3; PSA7, *Psma7*, proteasome subunit alpha
447 type-7; PYC, *Pcx*, pyruvate carboxylase, mitocondrial; PYRD2, Pyroxd2, pyridine
448 nucleotide-disulfide oxidoreductase domain-containing protein 2; TERA, *Vcp*,
449 transitional endoplasmic reticulum ATPase; TXNDC5, *Txndc5*, thioredoxin domain-
450 containing protein 5.

451

References

[1] Day CP. Genetic and environmental susceptibility to non-alcoholic fatty liver disease. Dig Dis. 2010;28:255-60.

[2] Kantartzis K, Schick F, Haring HU, Stefan N. Environmental and genetic determinants of fatty liver in humans. Dig Dis. 2010;28:169-78.

[3] Tiniakos DG, Vos MB, Brunt EM. Nonalcoholic fatty liver disease: pathology and pathogenesis. Annu Rev Pathol. 2010;5:145-71.

[4] Musso G, Gambino R, Cassader M. Recent insights into hepatic lipid metabolism in non-alcoholic fatty liver disease (NAFLD). Prog Lipid Res. 2009;48:1-26.

[5] Lou-Bonafonte JM, Arnal C, Osada J. New genes involved in hepatic steatosis. Curr Opin Lipidol. 2011;22:159-64.

[6] Acin S, Navarro MA, Perona JS, Surra JC, Guillen N, Arnal C, et al. Microarray analysis of hepatic genes differentially expressed in the presence of the unsaponifiable fraction of olive oil in apolipoprotein E-deficient mice. Br J Nutr. 2007;97:628-38.

[7] Assy N, Nassar F, Nasser G, Grosovski M. Olive oil consumption and non-alcoholic fatty liver disease. World J Gastroenterol. 2009;15:1809-15.

[8] Arbones-Mainar JM, Ross K, Rucklidge GJ, Reid M, Duncan G, Arthur JR, et al. Extra virgin olive oils increase hepatic fat accumulation and hepatic antioxidant protein levels in APOE-/- mice. J Proteome Res. 2007;6:4041-54.

[9] Covas MI, Ruiz-Gutiérrez V, de la Torre R, Kafatos A, Lamuela-Raventós RM, Osada J, et al. Minor Components of Olive Oil: Evidence to Date of Health Benefits in Humans. Nutrition Reviews. 2006;64:s20-s30.

[10] Lou-Bonafonte JM, Arnal C, Navarro MA, Osada J. Efficacy of bioactive compounds from extra virgin olive oil to modulate atherosclerosis development. Mol Nutr Food Res. 2012:In Press.

[11] Perona JS, Cabello-Moruno R, Ruiz-Gutierrez V. The role of virgin olive oil components in the modulation of endothelial function. J Nutr Biochem. 2006;17:429-45.

481 [12] Konstantinidou V, Covas MI, Munoz-Aguayo D, Khymenets O, de la Torre R,
482 Saez G, et al. In vivo nutrigenomic effects of virgin olive oil polyphenols within
483 the frame of the Mediterranean diet: a randomized controlled trial. FASEB J.
484 2010;24:2546-57.

485 [13] Owen RW, Mier W, Giacosa A, Hull WE, Spiegelhalder B, Bartsch H. Phenolic
486 compounds and squalene in olive oils: the concentration and antioxidant potential
487 of total phenols, simple phenols, secoiridoids, lignansand squalene. Food Chem
488 Toxicol. 2000;38:647-59.

489 [14] Murkovic M, Lechner S, Pietzka A, Bratacos M, Katzogiannos E. Analysis of
490 minor components in olive oil. J Biochem Biophys Methods. 2004;61:155-60.

491 [15] Smith TJ. Squalene: potential chemopreventive agent. Expert Opin Investig Drugs.
492 2000;9:1841-8.

493 [16] Gylling H, Miettinen TA. Postabsorptive metabolism of dietary squalene.
494 Atherosclerosis. 1994;106:169-78.

495 [17] Aguilera Y, Dorado ME, Prada FA, Martinez JJ, Quesada A, Ruiz-Gutierrez V.
496 The protective role of squalene in alcohol damage in the chick embryo retina. Exp
497 Eye Res. 2005;80:535-43.

498 [18] Ramírez-Torres A, Gabás C, Barranquero C, Martínez- Beamonte R, Fernández-
499 Juan M, Navarro MA, et al. Squalene: Current Knowledge and Potential
500 Therapeutical Uses. First edition ed. New York: NOVA; 2010.

501 [19] Guillen N, Acin S, Navarro MA, Perona JS, Arbones-Mainar JM, Arnal C, et al.
502 Squalene in a sex-dependent manner modulates atherosclerotic lesion which
503 correlates with hepatic fat content in apoE-knockout male mice. Atherosclerosis.
504 2008;197:72-83.

505 [20] Sarria AJ, Surra JC, Acin S, Carnicer R, Navarro MA, Arbones-Mainar JM, et al.
506 Understanding the role of dietary components on atherosclerosis using genetic
507 engineered mouse models. Front Biosci. 2006;11:955-67.

508 [21] Mensenkamp AR, Van Luyn MJ, Havinga R, Teusink B, Waterman IJ, Mann CJ,
509 et al. The transport of triglycerides through the secretory pathway of hepatocytes
510 is impaired in apolipoprotein E deficient mice. J Hepatol. 2004;40:599-606.

511 [22] Guillen N, Navarro MA, Arnal C, Noone E, Arbones-Mainar JM, Acin S, et al.
512 Microarray analysis of hepatic gene expression identifies new genes involved in
513 steatotic liver. Physiol Genomics. 2009;37:187-98.

514 [23] Arbones-Mainar JM, Navarro MA, Guzman MA, Arnal C, Surra JC, Acin S, et al.
515 Selective effect of conjugated linoleic acid isomers on atherosclerotic lesion
516 development in apolipoprotein E knockout mice. Atherosclerosis. 2006;189:318-
517 27.

518 [24] Arbones-Mainar JM, Navarro MA, Acin S, Guzman MA, Arnal C, Surra JC, et al.
519 Trans-10, cis-12- and cis-9, trans-11-conjugated linoleic acid isomers selectively
520 modify HDL-apolipoprotein composition in apolipoprotein E knockout mice. J
521 Nutr. 2006;136:353-9.

522 [25] Hotamisligil GS. Endoplasmic reticulum stress and atherosclerosis. Nat Med.
523 2010;16:396-9.

524 [26] Cnop M, Foufelle F, Velloso LA. Endoplasmic reticulum stress, obesity and
525 diabetes. Trends Mol Med. 2012;18:59-68.

526 [27] Fu S, Yang L, Li P, Hofmann O, Dicker L, Hide W, et al. Aberrant lipid
527 metabolism disrupts calcium homeostasis causing liver endoplasmic reticulum
528 stress in obesity. Nature. 2011;473:528-31.

529 [28] Fu S, Watkins SM, Hotamisligil GS. The role of endoplasmic reticulum in hepatic
530 lipid homeostasis and stress signaling. Cell Metab. 2012;15:623-34.

531 [29] Osada J, Aylagas H, Sanchez-Prieto J, Sanchez-Vegazo I, Palacios-Alaiz E.
532 Isolation of rat liver lysosomes by a single two-phase partition on
533 dextran/polyethylene glycol. Anal Biochem. 1990;185:249-53.

534 [30] Barcelo-Batllori S, Kalko SG, Esteban Y, Moreno S, Carmona MC, Gomis R.
535 Integration of DIGE and bioinformatics analyses reveals a role of the antiobesity
536 agent tungstate in redox and energy homeostasis pathways in brown adipose
537 tissue. Mol Cell Proteomics. 2008;7:378-93.

538 [31] Ramirez-Torres A, Barcelo-Batllori S, Fernandez-Vizarra E, Navarro MA, Arnal
539 C, Guillen N, et al. Proteomics and gene expression analyses of mitochondria
540 from squalene-treated apoE-deficient mice identify short-chain specific acyl-CoA

541 dehydrogenase changes associated with fatty liver amelioration. J Proteomics.
542 2012;75:2563-75.

543 [32] Bustin SA. Why the need for qPCR publication guidelines?--The case for MIQE.
544 Methods. 2009/12/23 ed2010. p. 217-26.

545 [33] Livak KJ, Schmittgen TD. Analysis of relative gene expression data using real-
546 time quantitative PCR and the 2(-Delta Delta C(T)) Method. Methods.
547 2001;25:402-8.

548 [34] Surra JC, Guillen N, Barranquero C, Arbones-Mainar JM, Navarro MA, Gascon S,
549 et al. Sex-dependent effect of liver growth factor on atherosclerotic lesions and
550 fatty liver disease in apolipoprotein E knockout mice. Histol Histopathol.
551 2010;25:609-18.

552 [35] Mi H, Dong Q, Muruganujan A, Gaudet P, Lewis S, Thomas PD. PANTHER
553 version 7: improved phylogenetic trees, orthologs and collaboration with the Gene
554 Ontology Consortium. Nucleic Acids Res. 2009;38:D204-10.

555 [36] Gygi SP, Rochon Y, Franza BR, Aebersold R. Correlation between protein and
556 mRNA abundance in yeast. Mol Cell Biol. 1999;19:1720-30.

557 [37] Kim SC, Sprung R, Chen Y, Xu Y, Ball H, Pei J, et al. Substrate and functional
558 diversity of lysine acetylation revealed by a proteomics survey. Mol Cell.
559 2006;23:607-18.

560 [38] Villen J, Beausoleil SA, Gerber SA, Gygi SP. Large-scale phosphorylation analysis
561 of mouse liver. Proc Natl Acad Sci U S A. 2007;104:1488-93.

562 [39] Saudek CD, Frier BM, Liu GC. Plasma squalene: lipoprotein distribution and
563 kinetic analysis. J Lipid Res. 1978;19:827-35.

564 [40] De Roos B, Rucklidge G, Reid M, Pickard K, Navarro MA, Arbonés-Mainar JM,
565 et al. Divergent mechanisms of cis9, trans11-and trans10, cis12-conjugated
566 linoleic acid affecting insulin resistance and inflammation in apolipoprotein E
567 knockout mice: a proteomics approach. Faseb J. 2005;19:1746-8.

568 [41] Afman L, Muller M. Nutrigenomics: from molecular nutrition to prevention of
569 disease. J Am Diet Assoc. 2006;106:569-76.

570 [42] Olofsson SO, Boren J. Apolipoprotein B secretory regulation by degradation.
571 Arterioscler Thromb Vasc Biol. 2012;32:1334-8.

572 [43] Fujimoto M, Hayashi T, Su TP. The role of cholesterol in the association of
573 endoplasmic reticulum membranes with mitochondria. Biochem Biophys Res
574 Commun. 2012;417:635-9.

575 [44] Kornmann B, Osman C, Walter P. The conserved GTPase Gem1 regulates
576 endoplasmic reticulum-mitochondria connections. Proc Natl Acad Sci U S A.
577 2011;108:14151-6.

578 [45] Kim HS, Kim JM, Roh KB, Lee HH, Kim SJ, Shin YH, et al. Rat liver 10-
579 formyltetrahydrofolate dehydrogenase, carbamoyl phosphate synthetase 1 and
580 betaine homocysteine S-methytransferase were co-purified on Kunitz-type
581 soybean trypsin inhibitor-coupled sepharose CL-4B. J Biochem Mol Biol.
582 2007;40:604-9.

583 [46] Agrawal G, Joshi S, Subramani S. Cell-free sorting of peroxisomal membrane
584 proteins from the endoplasmic reticulum. Proc Natl Acad Sci U S A.
585 2011;108:9113-8.

586 [47] Yonekawa S, Furuno A, Baba T, Fujiki Y, Ogasawara Y, Yamamoto A, et al.
587 Sec16B is involved in the endoplasmic reticulum export of the peroxisomal
588 membrane biogenesis factor peroxin 16 (Pex16) in mammalian cells. Proc Natl
589 Acad Sci U S A. 2011;108:12746-51.

590 [48] Jessop CE, Watkins RH, Simmons JJ, Tasab M, Bulleid NJ. Protein disulphide
591 isomerase family members show distinct substrate specificity: P5 is targeted to
592 BiP client proteins. J Cell Sci. 2009;122:4287-95.

593 [49] Buddhan S, Sivakumar R, Dhandapani N, Ganesan B, Anandan R. Protective effect
594 of dietary squalene supplementation on mitochondrial function in liver of aged
595 rats. Prostaglandins Leukot Essent Fatty Acids. 2007;76:349-55.

596 [50] Jiang XC, Li Z, Liu R, Yang XP, Pan M, Lagrost L, et al. Phospholipid transfer
597 protein deficiency impairs apolipoprotein-B secretion from hepatocytes by
598 stimulating a proteolytic pathway through a relative deficiency of vitamin E and
599 an increase in intracellular oxidants. J Biol Chem. 2005;280:18336-40.

600 [51] Uchiyama S, Shimizu T, Shirasawa T. CuZn-SOD deficiency causes ApoB
601 degradation and induces hepatic lipid accumulation by impaired lipoprotein
602 secretion in mice. J Biol Chem. 2006;281:31713-9.

603 [52] Ni M, Lee AS. ER chaperones in mammalian development and human diseases.
604 FEBS Lett. 2007;581:3641-51.

605 [53] Flores-Diaz M, Higuita JC, Florin I, Okada T, Pollesello P, Bergman T, et al. A
606 cellular UDP-glucose deficiency causes overexpression of glucose/oxygen-
607 regulated proteins independent of the endoplasmic reticulum stress elements. J
608 Biol Chem. 2004;279:21724-31.

609 [54] Dhahbi JM, Mote PL, Tillman JB, Walford RL, Spindler SR. Dietary energy
610 tissue-specifically regulates endoplasmic reticulum chaperone gene expression in
611 the liver of mice. J Nutr. 1997;127:1758-64.

612 [55] Nakatani Y, Kaneto H, Kawamori D, Yoshiuchi K, Hatazaki M, Matsuoka TA, et
613 al. Involvement of endoplasmic reticulum stress in insulin resistance and diabetes.
614 J Biol Chem. 2005;280:847-51.

615 [56] Wang ZS, Lu FE, Xu LJ, Dong H. Berberine reduces endoplasmic reticulum stress
616 and improves insulin signal transduction in Hep G2 cells. Acta Pharmacol Sin.
617 2010;31:578-84.

618 [57] Kobayashi T, Iguchi T, Ohta Y. Abetalipoproteinemia induced by overexpression
619 of ORP150 in mice. Comp Med. 2007;57:247-54.

620 [58] Wang Y, Wu Z, Li D, Wang D, Wang X, Feng X, et al. Involvement of oxygen-
621 regulated protein 150 in AMP-activated protein kinase-mediated alleviation of
622 lipid-induced endoplasmic reticulum stress. J Biol Chem. 2011;286:11119-31.

623 [59] Bloks VW, Plosch T, van Goor H, Roelofsen H, Baller J, Havinga R, et al.
624 Hyperlipidemia and atherosclerosis associated with liver disease in ferrochelatase-
625 deficient mice. J Lipid Res. 2001;42:41-50.

626 [60] Song SH, Min BI, Lee JH, Cho KS. Chronological effects of atherogenic diets on
627 the aorta, liver and spleen of rabbits. J Korean Med Sci. 2000;15:413-9.

628 [61] Brea A, Mosquera D, Martin E, Arizti A, Cordero JL, Ros E. Nonalcoholic fatty
629 liver disease is associated with carotid atherosclerosis: a case-control study.
630 Arterioscler Thromb Vasc Biol. 2005;25:1045-50.

[62] Spanova M, Zweytick D, Lohner K, Klug L, Leitner E, Hermetter A, et al. Influence of squalene on lipid particle/droplet and membrane organization in the yeast Saccharomyces cerevisiae. Biochim Biophys Acta. 2012; 1821: 647-53

Fig. 1. Effects of squalene on hepatic steatosis in apoE- knockout male mice. Representative micrographs of control (A) and squalene-treated liver sections (B), bar denotes 50 µm. C) Changes in hepatic fat content expressed as percentage of surface occupied by lipid droplets in experimental groups (control and squalene, n=5, respectively). D) Average lipid droplet diameter of 100 droplets per mouse of both experimental groups were measured and expressed in µm. Mann–Whitney *U*-test was used for the statistical analyses. **, $P < 0.01$.

Fig. 2. Proteome analyses of microsomal fractions. A) Representative images of Cy2, Cy3, Cy5 and the overlap of the 3 dyes of 2-DE gels from apoE-ko mice. B) 2D preparative Coomassie-stained gel with 34 spots exhibiting statistically significant differences. Spot numbers correspond to proteins shown in Table 1. C) Spot pairs corresponding to up-regulated PDIA3, PDIA1 and down-regulated NDUS1 and FTCD.

Fig. 3. Gene ontology groupings using the PANTHER classification system (www.pantherdb.org). Classification of the identified changed proteins according to A) biological processes and B) molecular functions.

Fig. 4. Association analyses among liver fat content, hepatic mRNA and protein levels of control and squalene-treated apoE-deficient mice. A) Correlation analysis among liver fat content and % normalized spot volume, B) Correlation analysis among *Txndc5* mRNA level and liver fat content and C) correlation analysis among *Txndc*5 and other hepatic mRNA levels. Black squares denote chow-fed and grey triangles squalene-treated mice.

Table 1. List of spots and characterized proteins differentially expressed between squalene-treated and control animals in apoE-deficient mice.

Spot number[a]	Protein name	UniProt ID	UniProt entry name	Gene symbol	Mascot score[b]	Sequence coverage (%)	Peptides[c]	Ions score[d]	MW experimental	MW theoretical	pI experimental	pI theoretical
1	Glutathione S-transferase Mu 1	P10649	GSTM1	*Gstm1*	283	37	22	278	25	25.8	7.73	8.14
2	Non-specific lipid-transfer protein	P32020	NLTP	*Scp2*	542	28	26	534	50	59.1	7.17	7.16
3	Protein disulfide-isomerase A3	P27773	PDIA3	*Pdia3*	9025	76	494	9025	49	54.2	5.64	5.69
4	Ubiquinone biosynthesis protein COQ9, mitochondrial	Q8K1Z0	COQ9	*Coq9*	189	17	10	189	32	30.2	4.92	4.93
5	Catalase	P24270	CATA	*Cat*	875	45	61	795	49	59.6	4.5	7.72
6	Thioredoxin domain-containing protein 5	Q91W90	TXNDC5	*Txndc5*	62	18	9	9	43	43.0	4.97	5.19
7	Phenazine biosynthesis-like domain-containing protein 2	Q9CXN7	PBLD2	*Pbld2*	606	48	20	594	31	31.9	4.99	5.19
8	Major urinary proteins 11 and 8	P04938	MUP8	*Mup8*	91	53	14	14	18	17	4.67	4.74
9	Glutathione S-transferase Mu 1	P10649	GSTM1	*Gstm1*	170	33	14	165	25	25.8	7.89	8.14
10	Protein disulfide-isomerase A3	P27773	PDIA3	*Pdia3*	112	39	27	29	49	54.2	5.54	5.69
11	Calcium-binding mitochondrial carrier protein Aralar2	Q9QXX4	CMC2	*Slc25a 13*	768	35	42	767	82	74.4	7.2	8.77
	Peroxisomal acyl-coenzyme A oxidase 1	Q9R0H0	ACOX1	*Acox1*	209	13	8	209	82	74.6	7.2	8.64
12	Enoyl-CoA hydratase	Q8BH95	ECHM	*Echs1*	388	28	30	383	27	28.5	7.92	7.78

	Proteasome subunit alpha type-7	Q9Z2U0	PSA7	*Psma7*	376	41	13	364	27	27.7	7.92	8.59
	Protein NipSnap homolog 1	O55125	NIPS1	*Nipsnap1*	248	27	8	248	27	33.3	7.92	9.48
13	Liver carboxylesterase 31	Q63880	EST31	*Ces3a*	224	15	9	224	54	60.0	7.9	5.78
	ATP synthase subunit alpha, mitochondrial	Q03265	ATPA	*Atp5a1*	283	19	12	282	54	55.3	7.9	8.28
	Pyridine nucleotide-disulfide oxidoreductase domain-containing protein 2	Q3U4I7	PYRD2	*Pyroxd2*	210	17	9	209	54	62.7	7.9	8.22
14	ATP synthase subunit beta, mitochondrial	P56480	ATPB	*Atp5b*	492	23	12	492	40	51.7	4.86	4.99
15	Arginase-1	Q61176	ARGI1	*Arg1*	109	51	21	5	38	34.8	6.45	6.52
16	Calreticulin	P14211	CALR	*Calr*	168	27	13	90	54	46.3	4.20	4.33
17	Protein disulfide-isomerase A3	P27773	PDIA3	*Pdia3*	612	51	40	356	49	54.2	5.45	5.69
18	Enoyl-CoA hydratase, mitochondrial	Q8BH95	ECHM	*Echs1*	306	27	21	305	26	28.5	7.9	7.78
	Proteasome subunit alpha type-7	Q9Z2U0	PSA7	*Psma7*	243	43	15	231	26	27.7	7.9	8.59
	Protein NipSnap homolog 1	O55125	NIPS1	*Nipsnap1*	237	32	9	237	26	33.3	7.9	9.48
19	Hypoxia up-regulated protein 1	Q9JKR6	HYOU1	*Hyou1*	4714	53	275	2578	158	107	4.96	5.06
20	78 kDa glucose-regulated protein	P20029	GRP78	*Hspa5*	145	28	20	58	78	70.5	4.7	5.01

21	Pyruvate carboxylase, mitochondrial	Q05920	PYC	*Pcx*	1140	39	59	1134	137	127.4	4.95	6.05
	Transitional endoplasmic reticulum ATPase	Q01853	TERA	*Vcp*	303	247	27	304	137	89.2	4.95	5.14
22	Propionyl-CoA carboxylase alpha chain, mitocondrial	Q91ZA3	PCCA	*Pcca*	700	45	36	683	76	74.5	5.75	6.04
23	Carbamoyl-phosphate synthase [ammonia], mitochondrial	Q8C196	CPSM	*Cps1*	1950	36	89	802	184	160.3	5.85	6.09
24	Carbamoyl-phosphate synthase [ammonia], mitochondrial	Q8C196	CPSM	*Cps1*	179	4	8	179	174	160.3	5.62	6.09
25	Carbamoyl-phosphate synthase [ammonia], mitochondrial	Q8C196	CPSM	*Cps1*	421	7	15	421	173	160.3	5.54	6.09
26	Carbamoyl-phosphate synthase [ammonia], mitochondrial	Q8C196	CPSM	*Cps1*	4670	64	306	2146	185	160.3	5.95	6.09
27	Actin, cytoplasmic 1	P60710	ACTB	*Actb*	143	40	19	58	42	41.7	5.03	5.29
28	Actin	P60710	ACTB	*Actb*	112	40	15	0	42	41.7	5.09	5.29
29	Aldehyde dehydrogenase family 1 member L1	Q8R0Y6	AL1L1	*Aldh1l1*	152	7	9	153	108	98.7	5.85	5.64
30	Calcium-binding mitochondrial carrier protein Aralar2	Q9QXX4	CMC2	*Slc25a 13*	660	31	35	660	71	74.5	7.39	8.77
	Peroxisomal acyl-coenzyme A oxidase 1	Q9R0H0	ACOX1	*Acox1*	197	9	5	198	71	74.6	7.50	8.64
31	NADH-ubiquinone oxidoreductase 75 kDa subunit	Q91VD9	NDUS1	*Ndufs1*	149	29	27	0	82	77.2	5.02	5.24

32	Protein disulfide-isomerase	P09103	PDIA1	*P4hb*	292	35	29	149	49	55.1	4.66	4.72
33	Formimidoyltransferase-cyclodeaminase	Q91XD4	FTCD	*Ftcd*	110	40	20	4	48	58.9	5.48	5.78
34	Glutamate dehydrogenase 1, mitochondrial	P26443	DHE3	*Glud1*	303	21	18	322	47	55.9	6.49	6.71
	ATP synthase subunit alpha, mitochondrial	Q03265	ATPA	*Atp5a1*	291	14	19	278	47	55.3	6.49	8.28

a. Spot numbers correspond to Figure 2B

b. Mascot score: Protein Mascot Score based on MS and MSMS data (Protein Summary report). Protein scores > 61 were significant ($p<0.05$). Values higher than 600 correspond to those identified by LC-MS/MS.

c. Number of matching peptides

d. Ion score: Mascot score which results from adding up individual MS/MS scores (Peptide Summary Report). Ion scores > 28 were significant ($p<0.05$

Table 2. Effect of squalene on proteins and their hepatic mRNA levels in apoE-ko mice.

Biological function	Protein name	Gene symbol	Protein fold change[a]	mRNA fold change[b]
Mitochondria				
Biosynthesis of oxalacetate	Pyruvate carboxylase	*Pcx*	1.3	2.6*
Biosynthesis of urea	Carbamoyl-phosphate synthase	*Cps1*	–1.9	1.7*
Carrier of aspartate	Aralar2	*Slc25a13*	1.4	1.9*
Carrier of aspartate	Aralar2	*Slc25a13*	–1.4	1.9*
Desamination of glutamate	Glutamate dehydrogenase 1	*Glud1*	–1.3	1.2
Electron transport	NADH-ubiquinone oxidoreductase 75 kDa subunit	*Ndufs1*	–1.4	1.4*
Electron transport	Ubiquinone biosynthesis protein COQ9	*Coq9*	1.5	1.2
Fatty acid catabolism	Enoyl-CoA hydratase	*Echs1*	1.4	1.0
Fatty acid catabolism	Propionyl-CoA carboxylase alpha	*Pcca*	1.3	1.4*
Generation of ATP	ATP synthase subunit alpha	*Atp5a1*	1.4	1.2
Generation of ATP	ATP synthase subunit alpha	*Atp5a1*	–1.3	1.2
Generation of ATP	ATP synthase subunit beta	*Atp5b*	1.4	1.3*
Peroxisomes				
Fatty acid oxidation	Acyl-coenzyme A oxidase 1	Acox1	–1.4	1.2
Fatty acid oxidation	Acyl-coenzyme A oxidase 1	*Acox1*	1.4	1.2
Inactivation of hydrogen peroxide	Catalase	*Cat*	1.5	1.6*
Endoplasmic reticulum				
Biosynthesis de amino acids	Phenazine biosynthesis-like domain-containing protein 2	*Pbld2*	1.5	1.2
Biosynthesis of urea	Arginase-1	*Arg1*	1.4	2.2*
Catabolism of proline	Protein disulfide-isomerase	*P4hb*	–1.3	1.2
Catabolism of histidine	Formimidoyltransferase-cyclodeaminase	*Ftcd*	–1.3	1.0
Catabolism of formyltetrahydrofolate	Aldehyde dehydrogenase 1L1	*Aldh1l1*	–1.4	2.1*
Conjugation of glutathione	Glutathione S-transferase Mu 1	*Gstm1*	1.7	1.1
Cytoskeleton	Actin	*Actb*	–1.5	0.9
Ester hydrolysis	Liver carboxylesterase 31	*Ces3a*	1.4	1.1
Intracellular vesicle transport	Protein NipSnap homolog 1	*Nipsnap1*	1.4	2.4*
Intracellular vesicle transport	Transitional endoplasmic reticulum ATPase	*Vcp*	1.3	1.0
Intracellular lipid transport	Non-specific lipid-transfer protein	*Scp2*	1.6	1.0
Intracellular lipid transport	Major urinary proteins 11 and 8	*Mup8*	1.5	1.0
Management of calcium storages	Calreticulin	*Calr*	1.3	1.2
Protein degradation	Proteasome subunit alpha type-7	*Psma7*	1.4	1.1
Protein folding	Protein disulfide-isomerase A3	*Pdia3*	1.6	1.3
Protein folding	78 kDa glucose-regulated protein	*Hspa5*	1.3	1.0
Protein insertion into membrane	Hypoxia up-regulated protein 1	*Hyou1*	1.3	2.0*
Redox homeostasis	Thioredoxin domain-containing protein 5	*Txndc5*	1.5	1.8*
Redox homeostasis in nucleotides	Pyridine nucleotide-disulfide oxidoreductase domain-containing protein 2	*Pyroxd2*	1.4	2.2*

[a] Positive and negative fold changes in spot expressions indicate up- and down-regulation of protein spots between squalene-treated (n=5) and control (n=5) animals.

[b] Fold changes in arbitrary fluorescence units normalized to the *Cyclophilin B* gene expression with the qPCR analysis. *P < 0.05

Table 3. Effect of squalene administration on hepatic mRNA levels in wild-type mice

	Control group (n=7)	Squalene group (n=7)
Arg1	1.0 ± 0.1	0.9 ± 0.2
Atp5b	1.0 ± 0.1	1.4 ± 0.3
Cat	1.2 ± 0.2	1.5 ± 0.2
Hyou1	1.1 ± 0.2	0.5 ± 0.2*
Nipsnap1	1.1 ± 0.2	1.2 ± 0.2
Pcca	1.1 ± 0.2	1.3 ± 0.2
Pcx	1.0 ± 0.1	0.9 ± 0.1
Pyroxd2	1.1 ± 0.1	1.2 ± 0.1
Txndc5	1.0 ± 0.1	0.8 ± 0.1

Results are expressed as mean ± SEM of arbitrary fluorescence units normalized to the *Cyclophilin B* gene expression with the qPCR analysis. Statistical analyses were done according to Mann–Whitney *U*-test.

Figure 1

Click here to download Figure: Figure 1new.ppt

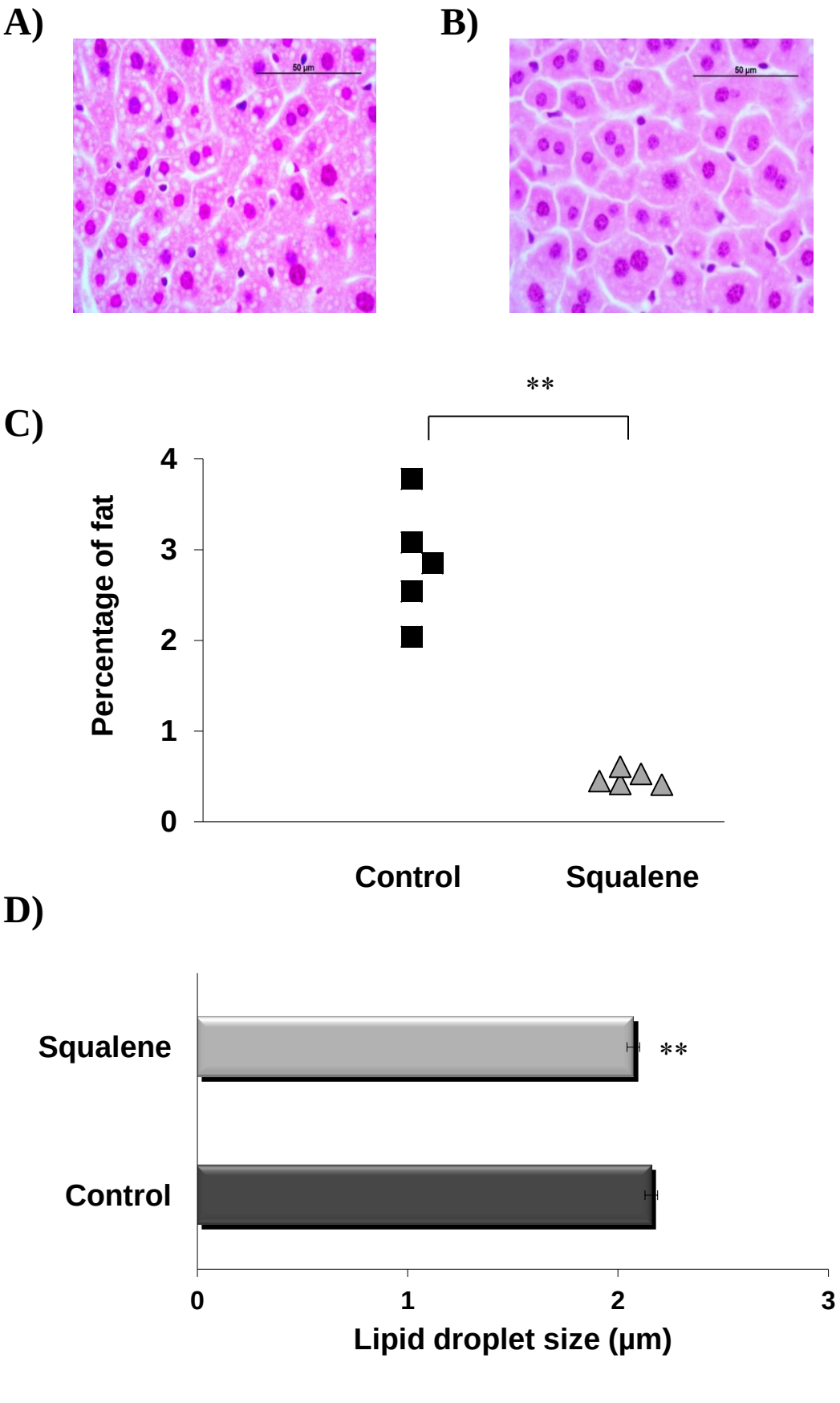

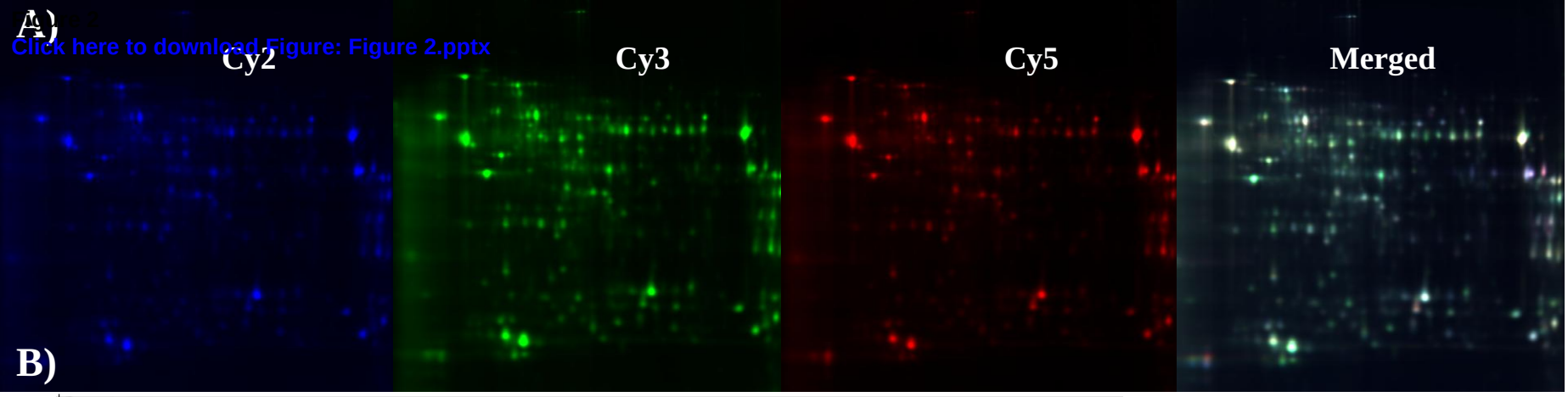

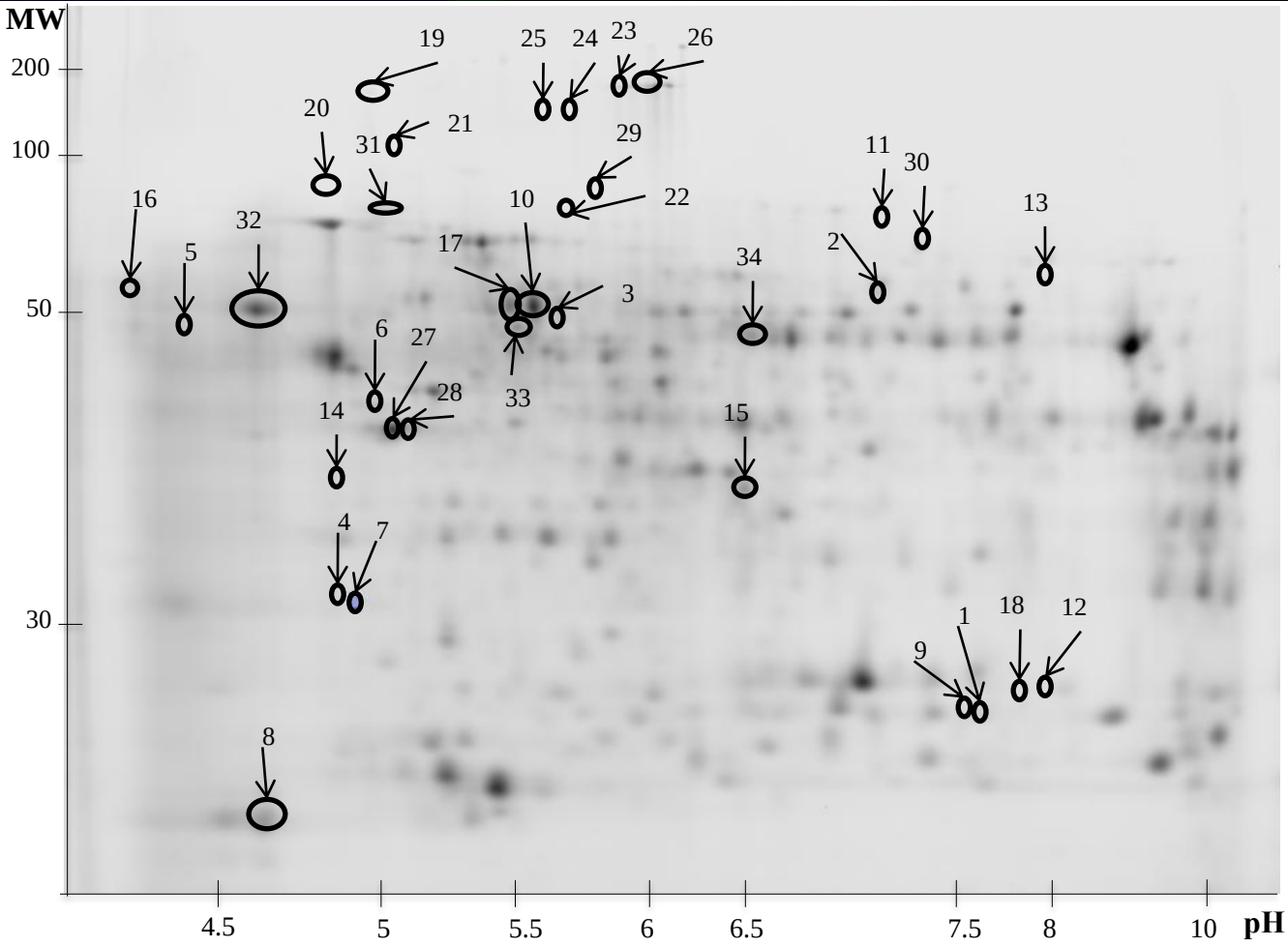

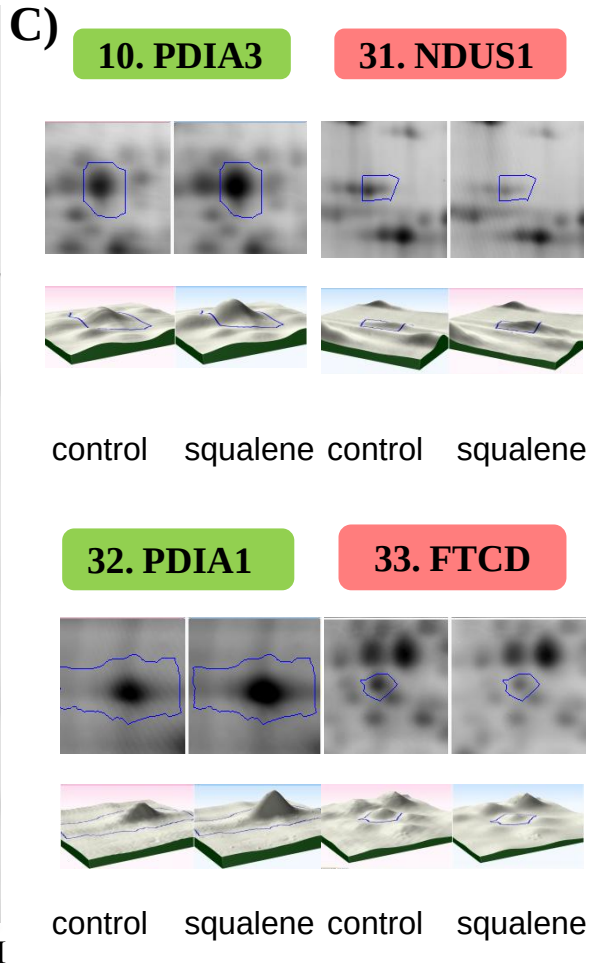

Figure 3

Click here to download Figure: Figure 3.ppt

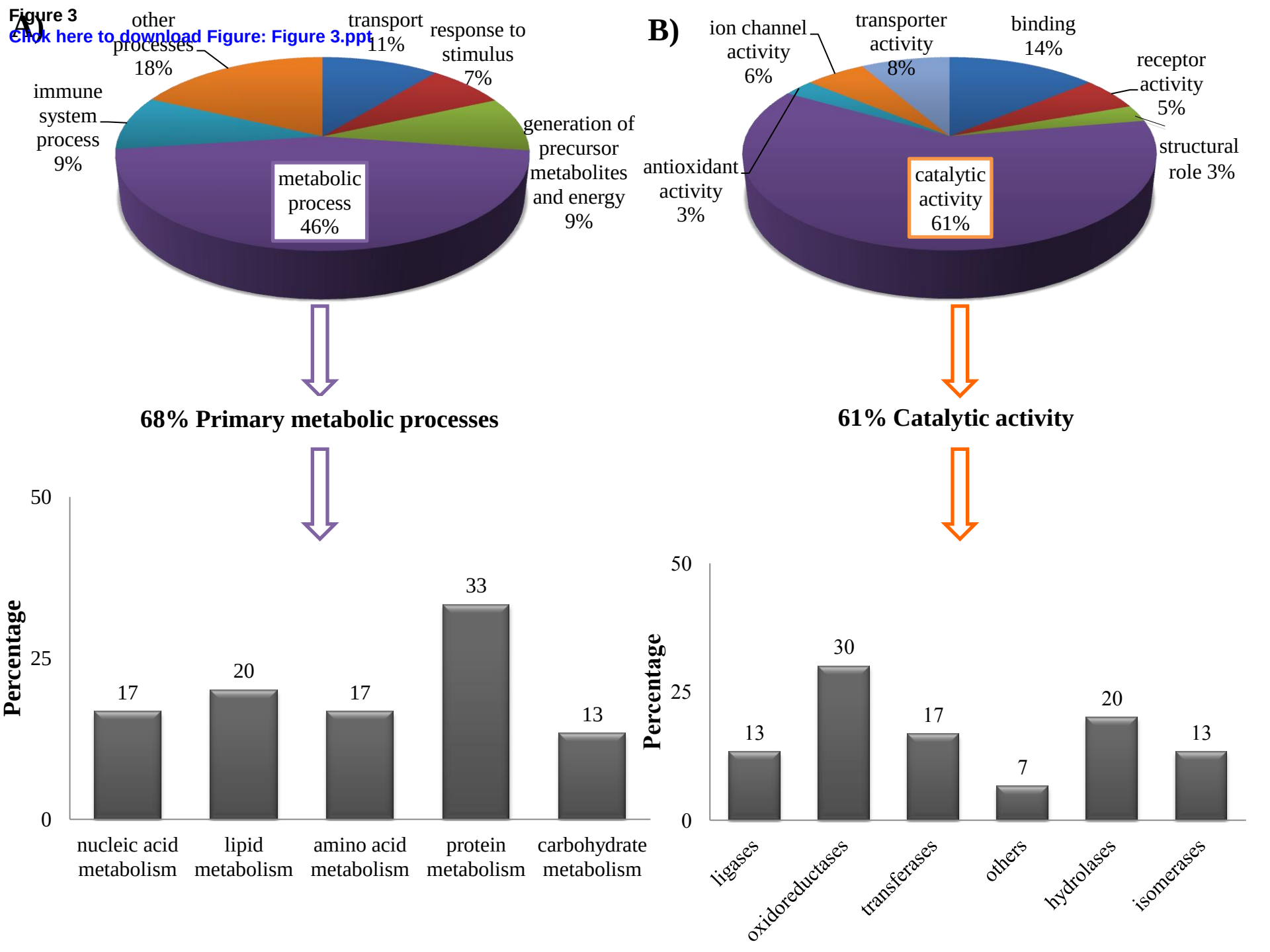

Figure 4

Click here to download Figure: Figure 4 new.ppt

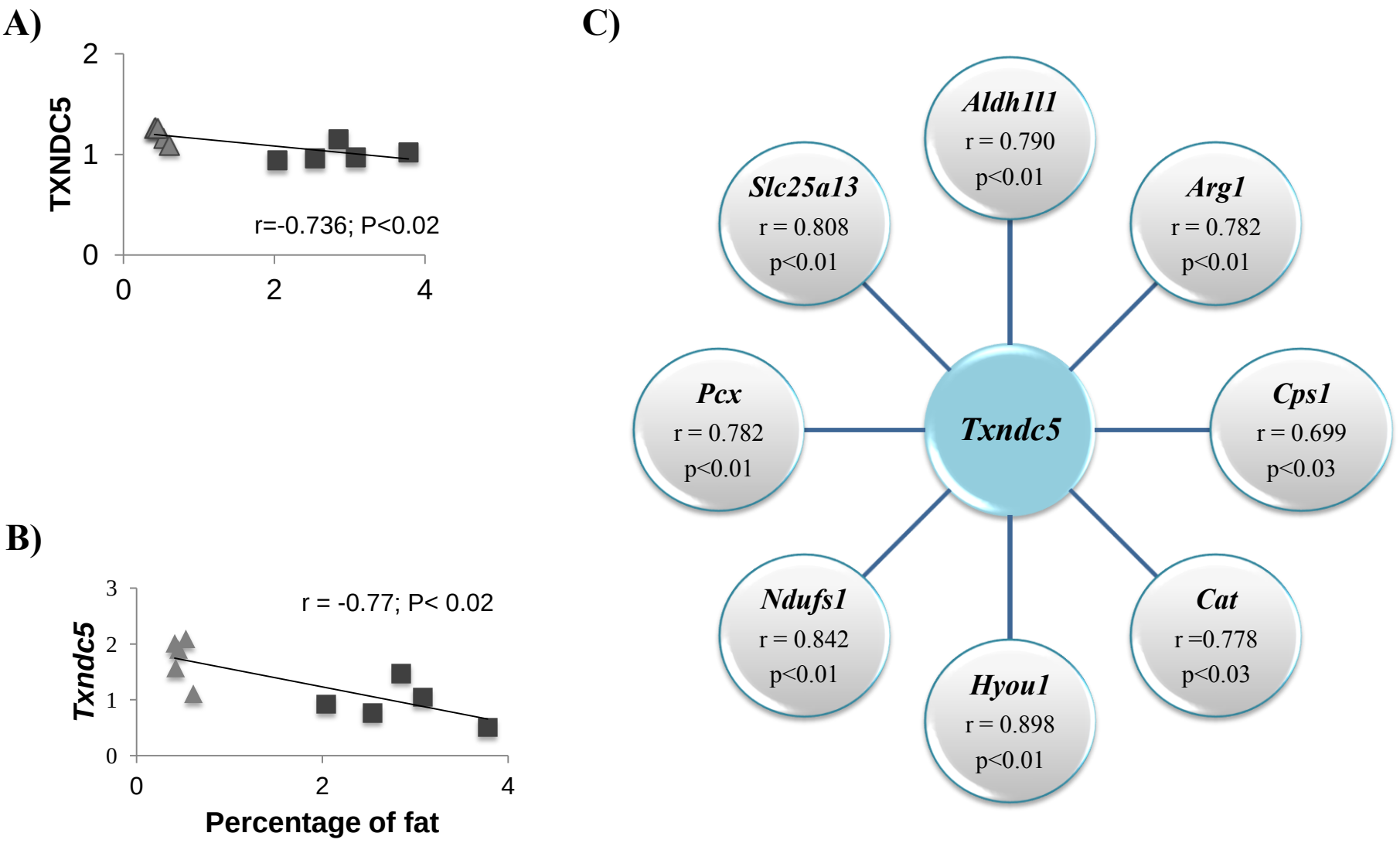

Supplementary Table 1

Click here to download Supplementary material: Supplementary Table 1.docx

Supplementary Table 2

Click here to download Supplementary material: Supplementary Table 2.xls